*36th EPS Conference on Plasma Phys. Sofia, June 29 - July 3, 2009 ECA Vol.**33E**, P-1.141 (2009)*

Rotation effect on geodesic ion Alfvén modes in hot tokamak plasmas

A.G. Elfimov, R.M.O.Galvão,

Institute of Physics, University of São Paulo, 05508-900, São Paulo, Brazil

M. Garcia-Munoz, V. Igochine, M. Maraschek and ASDEX Upgrade team

Max-Planck-Institute fuer Plasmaphysik, EURATOM Association, Garching, Germany

A new eigenmode driven by ICRH and named "sierpes" have been recently discovered in ASDEX Upgrade (AUG) tokamak [1], which appeared at the rational magnetic surface $q\approx1$ when the electron temperature was higher than some threshold of T_e>1.9eV. The mode has a frequency of 75-80 kHz, which does not depend on density or on toroidal magnetic field, and was detected by magnetic probes as well as soft X ray emission. That mode was associated with a loss of energetic ions from plasma core. In Ref 2, this mode is explained as results of the intersection of Alfvén wave continuum (AWC) with geodesic acoustic mode (GAM) at the rational magnetic surfaces below that some eigenmode may appear. In kinetic approach, the eigenmode appeared below AWC involves mainly ion oscillations that can be interpreted as Alfvén mode induced by geodesic ions (GIAM). The same effect is treated in Ref 3 as intersection of AWC and Beta Alfvén Eigenmode/GAM continuum. During NBI blips used for q profile determination in #22325 shot in AUG the sierpes mode is split in series of toroidal mode numbers (N=3, 4, 5) with different frequency (probably, due to rotation) as it is shown in the spectrogram of a central line of sight of the soft X-Ray (SXR) in Fig.1.

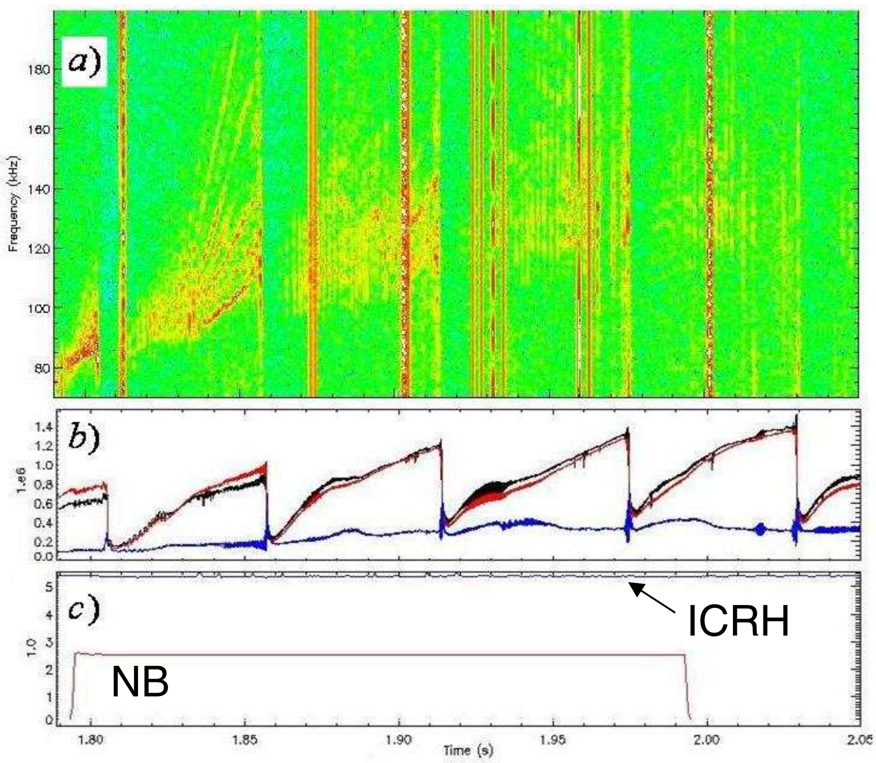

Fig.1. Spectrogram of J_53 SXR channel (a). Traces of J_53 (upper), J_52 of SXR (middle) central channels, and J_49 channel (below) showing inversion radius (b). ICRH and NB power (c).

Here, the rotation effect on GIAM at the rational magnetic surfaces is studied in the low frequency band in low aspect ratio tokamaks. Some kind of a drift kinetic equation [4] is used for toroidal plasmas with circular cross section ($R=R_0+r\cdot\cos\theta$, $z= r\cdot\cos\theta$), which are formed by the magnetic field with the toroidal and poloidal components, $B_\zeta= B_0 R_0/R$, $B_\vartheta=rB_\zeta/qR_0$, and $B_\theta<<B_\xi$. The equilibrium balance $\mathbf{j}^*\times\mathbf{B}/c\approx\nabla p$ is provided due to the diamagnetic current where the low plasma pressure $p=p_i+p_e$ is assumed, $8\pi p<<B^2$. The force-free non-compression plasma flux $div\mathbf{V}=0$ is proposed with the velocity $V=V_0R_0/R<<v_{Ti}$ orientated along magnetic field. The perturbed part of the distribution function f is represented as one wave mode proportional to linear perturbations of the electric and magnetic fields, $\tilde{E}_{1,2,3},\tilde{B}_{1,2,3}\sim\exp\left(i\left(N_z\zeta-\omega t\right)\right)$ where indexes 1,2,3 indicate the radial, binormal and parallel components. Quasi MHD approach for plasma conditions with the hot electrons, and warm ions, $v_{Te}=\sqrt{T_e/m_e}>>\omega R_0\geq v_{Ti}$, is used to eliminate E_3 from the drift kinetic equation for ions due to plasma quasi-neutrality, $e_iE_3=\frac{T_e}{R}\left(\frac{h_\vartheta}{r}\frac{\partial}{\partial\vartheta}\left(R...\right)+\mathrm{i}Nh_\zeta\right)\frac{\tilde{n}_i}{n_i}$. After Fourier series $\tilde{f}=\sum_M f_M\exp(\mathrm{i}M\vartheta)$, we obtain toroidal correction to cylindrical equation

$$
\begin{aligned}
f_{M\pm1}=&\frac{T_eF_0}{T_in_i}\frac{(\mathrm{v}_\parallel-V_0)k_{M\pm1}}{\left(\omega-\mathrm{v}_\parallel k_{M\pm1}\right)}\tilde{n}_{M\pm1}\pm\frac{h_\vartheta}{4R_0\mathrm{v}_\mathrm{T}^2}\frac{\mathrm{v}_\perp^2V_0-2\mathrm{v}_\parallel\mathrm{v}_\mathrm{T}^2}{\left(\omega-\mathrm{v}_\parallel k_{M\pm1}\right)}f_M^{\mathrm{cyl}}\\
&-\frac{e}{4m}\frac{F_0E_{1,M}}{\mathrm{v}_\mathrm{T}^2\omega_{c0}}\frac{h_\zeta}{R_0}\left[\frac{\mathrm{v}_\perp^2(M\pm1)[\mathrm{v}_\mathrm{T}^2-V_0(\mathrm{v}_\parallel-V_0)]\pm\mathrm{v}_\parallel(2\mathrm{v}_\parallel\mathrm{v}_\mathrm{T}^2-V_0\mathrm{v}_\perp^2)}{\left(\omega-\mathrm{v}_\parallel k_{M\pm1}\right)\mathrm{v}_\mathrm{T}^2}\right]\\
&-\mathrm{i}\frac{e}{4m}\frac{h_\zeta^2\mathrm{v}_\parallel(2\mathrm{v}_\parallel\mathrm{v}_\mathrm{T}^2-V_0\mathrm{v}_\perp^2)+\mathrm{v}_\perp^2[\mathrm{v}_\mathrm{T}^2-2V_0(\mathrm{v}_\parallel-V_0)]\left(1+\hat{D}_r\right)}{\omega_{c0}R_0\mathrm{v}_\mathrm{T}^2\left(\omega-\mathrm{v}_\parallel k_{M\pm1}\right)}\left(\frac{F_0E_{2,M}}{\mathrm{v}_\mathrm{T}^2}\right)
\end{aligned}
\tag{1}
$$

where $f_M^{\mathrm{cyl}}\approx-\frac{e}{2m}\frac{\mathrm{v}_\perp^2}{\omega\omega_{c0}}\left[\mathrm{i}\hat{D}_r\left(\frac{F_0E_{2,M}}{\mathrm{v}_\mathrm{T}^2}\right)+M\frac{F_0E_{1,M}}{\mathrm{v}_\mathrm{T}^2}\right]$, $k_M=M\,{}^{h_\vartheta}\!/_{r}+N\,{}^{h_\zeta}\!/_{R_0}$ is the parallel wave number, $\frac{\tilde{n}_{M\pm1}}{n_\mathrm{i}}=\frac{e_ih_\zeta}{m_iR\omega_c\omega}\chi_{M\pm1}\left(\pm\tau_{M\pm1}^{(1)}E_{1,M}+\mathrm{i}\hat{\tau}_{M\pm1}^{(2)}E_{2,M}\right)$, $\hat{D}_r=\frac{\partial}{\partial r}\left(r...\right)$ is the operator, and

$$
\tau_{\pm1}^{(1)}=z_{M\pm1}\left(\zeta_{M\pm1}\mp Mw_0\right)\mp\frac{M}{2}+\left[\left(\zeta_{M\pm1}z_{M\pm1}^2+\frac{\zeta_{M\pm1}}{2}\pm M(1-\zeta_{M\pm1}^2)w_0\right)Z(z_{M\pm1})\right],
$$

$$
\hat{\tau}_M^{(2)}=\left[z_{M\pm1}-\left(\frac{1}{2}+\zeta_{M\pm1}^2\right)Z(z_{M\pm1})\right]\zeta_{M\pm1}-\frac{\partial}{\partial r}\left[r\left(\frac{1}{2}+w_0\zeta_{M\pm1}+w_0(\zeta_{M\pm1}^2-\frac{1}{2})Z(z_{M\pm1})\right)...\right]
$$

$$
\chi_{M\pm1}=\left[{}^{T_i}\!/_{T_e}+\left(1+z_{M\pm1}Z(z_{M\pm1})\right)\right]^{-1},\ z_{\pm1}={}^{(\omega-Vk_{M\pm1})}\!/_{\sqrt{2}\mathrm{v}_\mathrm{Ti}k_{M\pm1}},\ k_{M\pm1}=\pm\,{}^{1}\!/_{R_0q_s},
$$

$w_0 = \dfrac{V}{\sqrt{2}\mathrm{v}_{\mathrm{Ti}}}$, $Z(z_{\pm1}) = \dfrac{1}{\sqrt{\pi}} \int\limits_{-\infty}^{\infty} \dfrac{dt \exp(-t^2)}{(t - z_{\pm1})}$ is the dispersion function, and $\zeta_{M\pm1} = z_{M\pm1}(V = 0)$.

After inserting of the $\tilde{f}_{M\pm1}^{(0e,i)}$ functions into the $\tilde{f}_{1,2}$–equations taken from Ref 4, which have to be averaged over magnetic surface with account of the ballooning effect, and integrating in the velocity space, we get the tensor-operator $\sum_p \tilde{\varepsilon}_{sp} E_{p,M} = \dfrac{4i\pi^2}{\omega} \sum_{e,i} e_i \int\limits_{-\infty}^{\infty} dv_\perp v_\perp^2 \int\limits_0^{\infty} dv_\| \oint \left(1 + \dfrac{r}{R}\cos\vartheta\right) f_s d\vartheta$.

Further, we calculate small toroidal corrections to a cylindrical dielectric tensor, and solve an eigenmode problem using quasi MHD approach for perpendicular electric field components

$$\frac{d}{dr}\left(rD\frac{dF}{dr}\right) + \left[\frac{dQ}{dr} - \frac{M^2 D}{r}\right]F = 0 \quad \text{where } F = rE_b, \quad Q = \left[M\, 2k_M \big/ R_0 q + M\, \omega_{ci} \big/ c_A^2 \left(\omega_i^* - \omega_e^*\right)\right]$$

are cylindrical functions [4]. The eigenmode is interpreted as Alfvén mode [2, 4] induced by geodesic ions (GIAM), which may appear below AWC described by equation

$$D = \frac{\omega^2}{c^2}\left(\frac{c^2}{c_A^2} + \varepsilon_{11}^{\mathrm{geo}}\right) - k_M^2 = 0, \quad \varepsilon_{11}^{\mathrm{geo}} = \sum_i \frac{\omega_{p\alpha}^2 h_\zeta^2 \mathrm{v}_{\mathrm{T}i}^2}{\omega_{ci}^2 R^2 \omega^2} \Psi\left(\frac{R_0 q\omega}{\sqrt{2}\mathrm{v}_{\mathrm{Ti}}}\right) \tag{2}$$

$$\Psi(\zeta) = -\chi\zeta\left[Z(\zeta)(2 + \zeta Z(\zeta))\left(\frac{1}{2} + 2\zeta(Mw_0 + \zeta + \zeta^3)\right) + 2(Mw_0 + \zeta + \zeta^3)\right.$$
$$\left. + 2Z(\zeta)\left[2Mw_0(1 - \zeta^4) + \zeta\left(\frac{1}{2} + \zeta^2 + \zeta^4\right)\right] - \zeta\left[2Mw_0(1 + 2\zeta^2) - \zeta^2(3 + 2\zeta^2)\right]\right],$$

where $\chi = \left[T_i \big/ T_e + (1 + \zeta Z(\zeta))\right]^{-1}$.

To demonstrate the importance of the kinetic effects, the geodesic frequency normalized on the ion circulation one $v_{Ti} \big/ R_0$ is found from *D*=0 implicit equation for any rational *q* at $k_M=0$.

The results are shown in Fig.2, where the frequency is plotted over rational *q* values for different the velocities ($V_0/\mathrm{v}_{\mathrm{Ti}}$=0, ±0.15). The plotted curves expanded in cold limit ($\omega R_0 q >> v_{Ti}$) can be presented by approximate equation $\omega_{\mathrm{geo}} \approx \dfrac{\mathrm{v}_{\mathrm{Ti}}}{R_0}\sqrt{\left(\dfrac{7}{2} + 1\big/q^2 + T_e\big/T_i q^2 + MV_0\big/2q\mathrm{v}_{\mathrm{Ti}}\right)}$. Dispersion curves shown in Fig.2 confirm that there is an electron temperature threshold [2], which also depends on rotation velocity. As a result, GIAM may be excited at the *q*≈1 rational surface only for the electron temperature higher then the ion one $(T_e \geq T_{\mathrm{i}})$ for the “positive” rotation ($V_0 M/q \geq 0$).

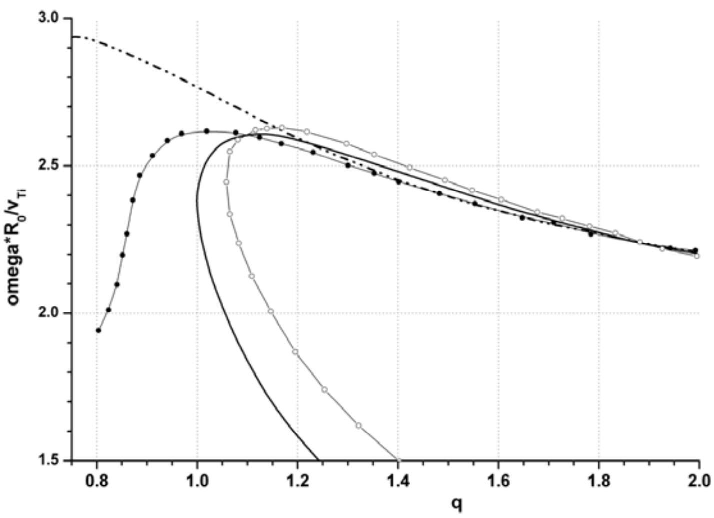

Fig.2. *Plot of the normalized geodesic frequency over rational q-factor for the temperature ratio, T_e /T_i =0.95, M=4, V=0 (solid line), V=±0.15v_{Ti} (black and open circles, respectively); T_e /T_i =1.2 and V=+0.15 v_{Ti}, M=9 (chain line).*

The conditions for existence of the GIAM eigenmodes localized at the rational surface r=r_s below the continuum minimum $(\omega = \omega_{\rm geo} - \delta\omega,)$, $(\delta\omega << \omega_{\rm geo})$ will be the same as the ones presented in Ref 4 instead of the geodesic frequency, which value should be calculated using directly eq (2). The dispersion curves demonstrate that the curve (solid line) touches the q=1 line at the frequency about 2.3 of the ion circulation frequency when rotation is low and electron temperature stays at the threshold. If rotation is slightly enhanced (due to NB injection, for example) the curve (black dots) moves to left but GIAM should stay at q=1 surface. In this case, the frequency of the mode has to be jump “up” or “down” abruptly. For the "down" case, ion Landau damping begins to be strong and the mode may disappear. For the “up” case, the mode dissipation stays small and the mode can propagate. That case may explain why the diagnostic NBI may trigger the splitting effect for the *sierpies* mode in the conditions of the 22325 shot shown in Fig.1. For the negative rotation V =-0.15v_{Ti}, and M=4, AWC minimum and GIAMs may appear at the q=1 surface only for high electron temperature $T_e \geq 1.5 T_{\rm i}$ and the dispersion curve will be the same as for T_e= 0.95T_i (V =0) shown in Fig 2.

Finally, we conclude that developed kinetic theory shows that the Alfvén wave continuum minimum is defined by geodesic effect of untapped ions, below which GIAM can be exited in specific conditions when the electron temperature is higher than some threshold for positive rotation, which may explain behavior of the sirpes modes in ASDEX Upgrade tokamak.

Authors are thankful to Dr. P. Lauber for helpful discussions.

[1] M.Garcia-Munoz, H.-U. Fahrbach, et al, *PRL*, 100, 055005 (2008).

[2] A.G. Elfimov, *Physics of Plasmas* **16**, 034501 (2009).

[3] F.Zonca and L.Chen, EPL, **83**, 35001 (2008).

[4] A.G. Elfimov, *Physics of Plasmas* **15**, 074503 (2008).